

# Metal Ions To Control the Morphology of Semiconductor Nanoparticles: Copper Selenide Nanocubes

Wenhua Li,<sup>‡</sup> Reza Zamani,<sup>‡,||</sup> Maria Ibáñez,<sup>†</sup> Doris Cadavid,<sup>‡</sup> Alexey Shavel,<sup>‡</sup> Joan Ramon Morante,<sup>†,‡</sup> Jordi Arbiol,<sup>||,§</sup> and Andreu Cabot<sup>\*,†,‡</sup>

<sup>‡</sup>Catalonia Energy Research Institute - IREC, Jardí de les Dones de Negre, 1, 08930 Sant Adria del Besos, Barcelona, Spain

<sup>||</sup>Institut de Ciència de Materials de Barcelona, ICMA-B-CSIC, Campus de la UAB, 08193 Bellaterra, Spain

<sup>†</sup>Departament d'Electrònica, Universitat de Barcelona, Martí i Franques 1, 08028 Barcelona, Spain

<sup>§</sup>Institució Catalana de Recerca i Estudis Avançats (ICREA), 08010 Barcelona, Spain

## Supporting Information

**ABSTRACT:** Morphology is a key parameter in the design of novel nanocrystals and nanomaterials with controlled functional properties. Here, we demonstrate the potential of foreign metal ions to tune the morphology of colloidal semiconductor nanoparticles. We illustrate the underlying mechanism by preparing copper selenide nanocubes in the presence of Al ions. We further characterize the plasmonic properties of the obtained nanocrystals and demonstrate their potential as a platform to produce cubic nanoparticles with different composition by cation exchange.

It is in large part through the surface that nanocrystals (NCs) interact with neighboring NCs and the medium. Catalytic, electronic, optoelectronic and thermoelectric performance of NCs and nanocrystalline materials strongly rely on the chemical and energy exchange in the form of ions, charge carriers or phonons that take place between NCs themselves and between NCs and the medium. In this sense, numerous applications depend on the organization of the NC last atomic layers. That is, on the type and ratio of the NC facets, i.e., its morphology.

Morphology also controls NC assembly into macroscopic superstructures. In this regard, a particularly interesting geometry for technological applications is that of cubes.<sup>1</sup> Nanocubes can maximize NC packing and produce highly compact films or bulk nanostructured materials. At the same time, nanocubes can form lattice-matched superstructures where all crystallographic domains are oriented in the same direction.<sup>2</sup> This may be an important asset in magnetic, electronic, optoelectronic, and thermoelectric applications, where charge carrier or phonon exchange is fundamental.

To control NC morphology, organic molecules that selectively bind to different NC facets are generally used. There are countless examples on the use of aliphatic chains with carboxylic acid, phosphonic acid and amine functional groups to control the morphology of elemental, binary, ternary, and quaternary nanoparticles.<sup>3</sup> Some metal ions have also been proved as efficient directors of NC morphology, especially for metal nanoparticles. A particularly illustrative example is that of Pt-based nanocubes. Tungsten,<sup>4</sup> iron,<sup>5</sup> cobalt,<sup>6</sup> and chromium<sup>7</sup> carbonyls and also iron chloride,<sup>8</sup> silver nitrate<sup>9</sup> and silver

acetylacetonate<sup>10</sup> have been used to produce Pt nanocubes by manipulating NC nucleation and growth rate in the different crystallographic directions. In many cases, these metal ions did not incorporate in the NC structure and were not detected on the surface or within the final NCs. They just catalyzed the nanocube formation, returning afterward to the solution or precipitating as a salt.

Previous studies on the use of foreign metal ions to control NC morphology were focused on metal NCs. However, because the underlying mechanism is a general one, we believe metal ions should be also included in our tool bench as potential morphology drivers of semiconductor NCs.

Here, we report an example of the influence of foreign metal ions to control the morphology of a chalcogenide semiconductor: Cu<sub>x</sub>Se. In particular, we detail a synthetic route to produce Cu<sub>x</sub>Se nanocubes by the incorporation of Al ions in the initial precursor solution. We also characterize the plasmonic properties of the new copper selenide geometry obtained and demonstrate the potential of the produced Cu<sub>x</sub>Se NCs to prepare nanocubes of other semiconductor chalcogenides by cation exchange. This is exemplified by preparing Ag<sub>2</sub>Se nanocubes.

We produced Cu<sub>x</sub>Se NCs by reacting CuCl with an excess of selenium precursor in the presence of hexadecylamine (HDA). In a typical preparation, 0.0495 g of CuCl (0.5 mmol, 99.99%, Aldrich), 5 mmol HDA (90% Aldrich) and 10 mL of octadecene (ODE, 90%, Aldrich) were introduced inside a four-neck flask and heated to 200 °C under argon flow until all precursors were dissolved. The yellowish transparent solution produced was maintained under Ar flow at 200 °C for an additional hour to remove oxygen, water and other low-boiling point impurities. Afterward, the solution was cooled to 180 °C and 4 mL of a 0.8 M ODE-Se solution was injected through a septum (detailed information on the selenium precursor preparation and the nanocrystal synthesis can be found in the Supporting Information, SI). The mixture was maintained at 180 °C for 5 min. Afterward, the solution was rapidly cooled down to room temperature. The NCs were isolated and purified using the standard solvent/nonsolvent precipitation/redispersion procedure. The reaction yield was around 80% for

Received: January 15, 2013

Published: March 7, 2013

all the synthesis here reported. Figure 1a shows a representative transmission electron microscopy (TEM) micrograph of the quasi-spherical  $\text{Cu}_x\text{Se}$  NCs obtained following the above-described procedure.

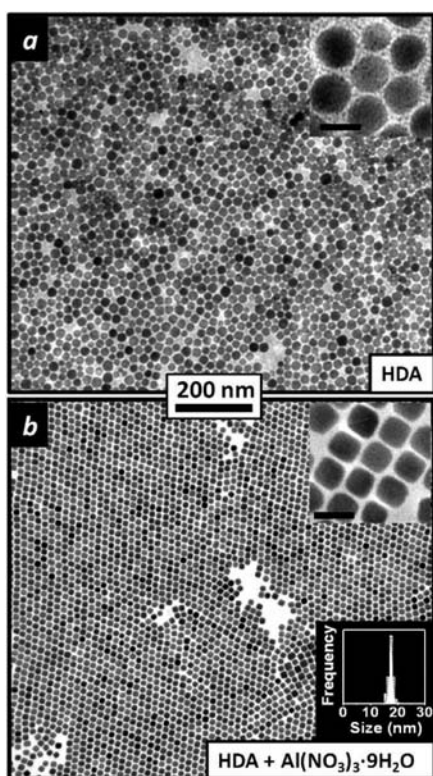


**Figure 1.** (a) TEM micrograph of quasi-spherical  $\text{Cu}_x\text{Se}$  NCs obtained by reacting  $\text{CuCl}$  with  $\text{ODE-Se}$  in the presence of  $\text{HDA}$  at  $180\text{ }^\circ\text{C}$ . (b) TEM micrograph and particle size distribution of  $\text{Cu}_x\text{Se}$  NCs obtained by reacting  $\text{CuCl}$  with  $\text{ODE-Se}$  in the presence of  $\text{HDA}$  and  $\text{Al}(\text{NO}_3)_3 \cdot 9\text{H}_2\text{O}$  at  $180\text{ }^\circ\text{C}$ . Scale bars of inset TEM micrographs correspond to  $20\text{ nm}$ .

In an attempt to prepare  $\text{CuAlSe}_2$  NCs, we added  $\text{Al}(\text{NO}_3)_3 \cdot 9\text{H}_2\text{O}$  in the precursor solution. All other parameters were maintained the same. Figure 1b shows a representative TEM micrograph of the NCs obtained in the presence of  $0.1\text{ mmol}$  of  $\text{Al}(\text{NO}_3)_3$ . When reacting  $\text{CuCl}$  with the  $\text{ODE-Se}$  solution for  $5\text{ min}$  in the presence of  $\text{HDA}$  and  $\text{Al}(\text{NO}_3)_3$ , nanocubes with very low size dispersions,  $\sim 5\%$ , were systematically obtained (Figure 1b, inset, SI).

To our surprise and initial disappointment, energy dispersive X-ray (EDX) analysis inside a scanning electron microscope (SEM) showed the presence of no Al in the nanocube sample. From the EDX analysis, the sample composition matched approximately to  $\text{Cu}_3\text{Se}_2$ . Electron energy loss spectroscopy (EELS) further confirmed the absence of Al and the NC composition to be  $\text{Cu}_3\text{Se}_2$ . Single particle EELS analyses showed NCs to have a  $\text{Cu}:\text{Se}$  ratio  $3:2$  with a composition distribution from particle to particle within the technique uncertainty. Single particle EELS elemental maps further showed that the NC composition was highly homogeneous within each particle.

To determine the influence of  $\text{NO}_3^-$  and  $\text{Al}^{3+}$  ions on the  $\text{Cu}_3\text{Se}_2$  NC growth, various control experiments were carried out. Figure 2 displays the TEM micrographs of the NCs obtained from the reaction of  $\text{CuCl}$  with the  $\text{ODE-Se}$  solution

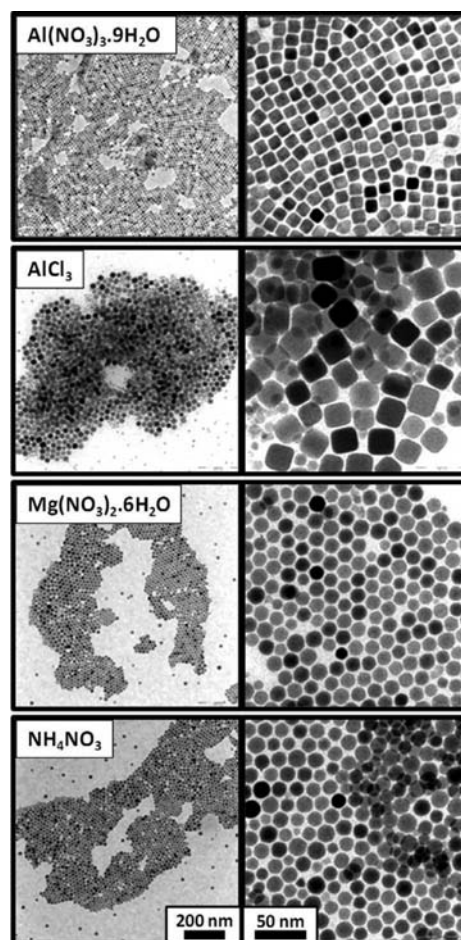


**Figure 2.** TEM micrographs of  $\text{Cu}_3\text{Se}_2$  NCs obtained in the presence of  $\text{HDA}$  and different salts, as noted.

in the presence of  $\text{HDA}$  and different salts:  $\text{Al}(\text{NO}_3)_3 \cdot 9\text{H}_2\text{O}$ ,  $\text{Mg}(\text{NO}_3)_2 \cdot 6\text{H}_2\text{O}$ ,  $\text{AlCl}_3$ ,  $\text{NH}_4\text{NO}_3$ .  $\text{Cu}_3\text{Se}_2$  nanocubes were only obtained in the presence of  $\text{Al}(\text{NO}_3)_3 \cdot 9\text{H}_2\text{O}$  and  $\text{AlCl}_3$ . The NCs obtained in the presence of  $\text{AlCl}_3$  were sensibly worse in terms of size distribution than those obtained with  $\text{Al}(\text{NO}_3)_3 \cdot 9\text{H}_2\text{O}$ . The presence of  $\text{HDA}$  and the purity of the  $\text{Se}$  precursor solution were also demonstrated as essential to obtain nanoparticles with narrow size distributions. In particular, the  $\text{Se}$  source was very sensitive to preparation.<sup>11</sup> We are currently studying in detail the influence of the  $\text{Se}$  precursor preparation method on the morphology of the produced  $\text{Cu}_3\text{Se}_2$  NCs.

Figure 3 displays TEM micrographs of the NCs extracted at different reaction times from a single batch. Initial  $\text{Cu}_3\text{Se}_2$  NCs displayed similar sizes and narrow size distributions as in the final product but were characterized by quasi-spherical

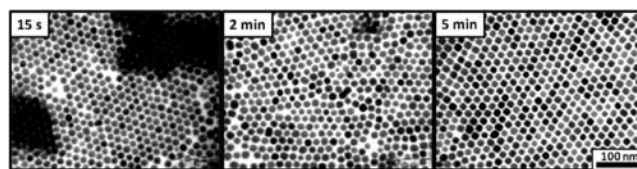


**Figure 3.** TEM micrographs of  $\text{Cu}_3\text{Se}_2$  NCs obtained at successively higher reaction times.



geometries. NCs morphology evolved from quasi-spherical to cubic within a few minutes of reaction.

The identification of copper selenide crystallographic phases is particularly difficult. Copper selenides exist in a wide variety of compositions and crystallographic systems, including orthorhombic, monoclinic, and cubic.<sup>12</sup> Figure 4 shows the

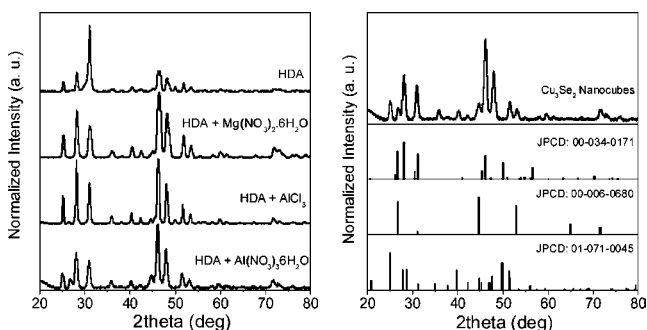


**Figure 4.** XRD patterns of the  $\text{Cu}_3\text{Se}_2$  NCs obtained in the presence of HDA and different salts. As a reference, the peak position of various copper selenide phases is also represented: klockmannite hexagonal  $\text{CuSe}$  JPCD, 00-034-0171; berzelianite cubic  $\text{Cu}_{2-x}\text{Se}$  JPCD, 00-006-0680; umangite tetragonal  $\text{Cu}_3\text{Se}_2$  JPCD, 01-071-0045.

X-ray diffraction (XRD) pattern of the nanoparticles prepared in the presence of HDA and different salts. X-ray diffraction analysis evidenced that the crystallographic structure of the  $\text{Cu}_3\text{Se}_2$  NCs was not substantially modified by the presence of  $\text{Al}^{3+}$  ions in the precursor solution. From the NC composition obtained by EDX and EELS analysis, we anticipated the NCs to display the tetragonal umangite crystal structure. However, XRD patterns did not exactly match the umangite reference pattern (JCPDF: 01-071-0045). XRD patterns obtained did not exactly match any of the previously reported structures as shown in Figure 4.

Figure 5 shows HRTEM micrographs and the corresponding power spectrum obtained by aligning the incident electron

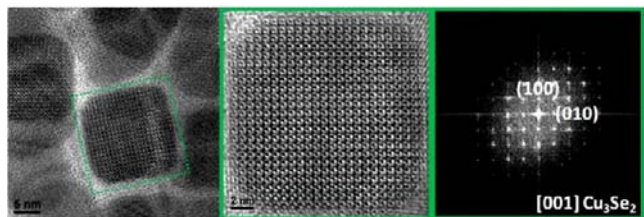


**Figure 5.** HRTEM micrographs and corresponding power spectrum of  $\text{Cu}_3\text{Se}_2$  nanocubes.

beam perpendicular to one of the square facets of a  $\text{Cu}_3\text{Se}_2$  cube. The crystal structure obtained from HRTEM could be associated to the umangite tetragonal phase (S.G.:  $P4_21m$ ) with lattice parameters ( $a = b = 7.2 \text{ \AA}$ ;  $c = 2a$ ). However the cell parameters obtained from the power spectrum analyses were significantly different from those of the reported umangite phase. Otherwise, the crystal structure could be identified as orthorhombic with cell parameters  $a = 7.2 \text{ \AA}$ ,  $b = 7.3 \text{ \AA}$  and  $c = 14.4\text{--}14.5 \text{ \AA}$ . However, such crystal phase has not been previously reported, and attending to the very small difference between  $a$  and  $b$  cell parameters, it is more reasonably to associate the crystal structure to a quasi-tetragonal phase with  $c$  parameter being  $2a$  ( $a = b$ ;  $c = 2a$ ). Still, the formation of a

tetragonal structure with double cell parameter along  $c$  suggests some ordering along the  $z$ -axis.

From the experimental results obtained, it is evident that  $\text{Al}^{3+}$  ions had a strong influence on the  $\text{Cu}_3\text{Se}_2$  NC morphology. Because the cubic morphology was obtained after a few minutes of reaction time, after NCs reached an equilibrium with the monomer concentration in solution (Figure 3), it is clear that nanocubes were formed during ripening due to a stability differential between the  $\{111\}$  and the  $\{100\}$  and  $\{001\}$  facets of the  $\text{Cu}_3\text{Se}_2$  tetragonal-like structure. On the other hand, the chemical analysis of the final nanoparticles demonstrated that  $\text{Al}^{3+}$  ions did not incorporate to the  $\text{Cu}_3\text{Se}_2$  crystal structure or surface facets in the used synthesis conditions. Adding both experimental observations together, we speculate that the role of  $\text{Al}^{3+}$  ions is more probably to promote the crystal growth in a specific direction instead of stabilizing a particular facet. We hypothesize that  $\text{Al}^{3+}$  ions block the binding of HDA to the  $\{111\}$  facets. Then, during the ripening regime, while  $\{100\}$  and  $\{001\}$  facets capped by HDA are stable toward the incorporation or dissolution of Cu and Se ions,  $\{111\}$  facets, possibly terminated by  $\text{Al}^{3+}$  ions with a fast dynamic solvation, are subject to a relatively fast exchange of Cu and Se ions with the solution. Thus,  $\{111\}$  facets tend to disappear with the reaction time and  $\{100\}$  and  $\{001\}$  faceted nanocubes are formed. Again, the nanoparticle quality and morphology were very sensitive to the purity of the Se precursor solution. Thus, ODE-Se must play an important role which remains to be elucidated in the global mechanism of  $\text{Cu}_3\text{Se}_2$  NC size and shape control.

Copper selenides are usually p-type semiconductors with band gaps in the range 1.0–2.0 eV.<sup>13</sup> Their p-type character is associated to the presence of copper vacancies in the lattice, which makes their carrier concentration and transport properties strongly dependent on its composition. Copper selenides also display composition-dependent plasmonic light scattering in the Near-Infrared spectral Region (NIR).<sup>14</sup> Their band gap in the visible part of the spectrum and their plasmonic properties make copper selenides valuable materials in optoelectronic and plasmonic applications.

Figure 6a shows the UV–vis spectra of colloidal  $\text{Cu}_3\text{Se}_2$  nanocubes in tetrachloroethylene. A plasmon peak was clearly observed. The maximum of the peak red-shifted from 940 to 1110 nm when reducing the NCs with a  $\text{Li}(\text{C}_2\text{H}_5)_3\text{BH}$  solution in tetrahydrofuran, proving its strong composition dependence.

As pointed out above, nanocubes have a convenient geometry for technological applications as they can maximize

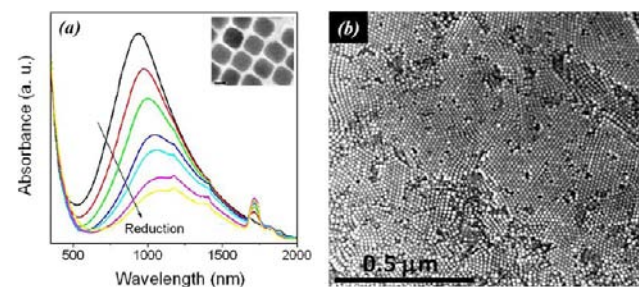


**Figure 6.** (a) Evolution of the absorption spectra of  $\text{Cu}_3\text{Se}_2$  nanocubes in tetrachloroethylene when chemically reduced. Each step from the black toward the yellow spectrum corresponds to an addition of  $50 \mu\text{L}$  of a 0.02 M  $\text{Li}(\text{C}_2\text{H}_5)_3\text{BH}$  solution in tetrahydrofuran. (b) SEM micrograph of an assembly of  $\text{Cu}_3\text{Se}_2$  nanocubes.

NC packing and produce highly compact films or bulk nanostructured materials (Figure 6b). Because of their advantageous morphology, we further used the  $\text{Cu}_3\text{Se}_2$  nanocubes as a platform to produce other semiconductor nanocubes by cation exchange. Figure 7 shows a representative

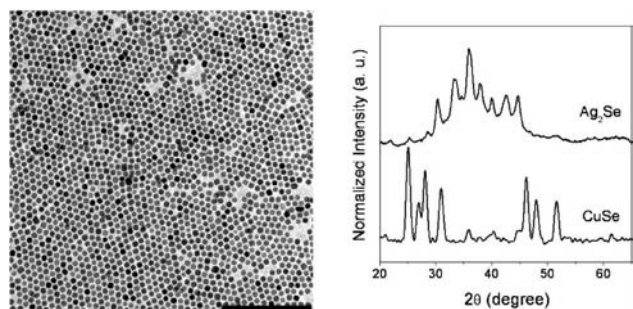


**Figure 7.** TEM micrograph and XRD pattern of the  $\text{Ag}_2\text{Se}$  nanocubes obtained by cation exchange from  $\text{Cu}_3\text{Se}_2$  nanocubes. Scale bar corresponds to 200 nm.

TEM micrograph and the corresponding XRD pattern of the  $\text{Ag}_2\text{Se}$  nanocubes obtained by cation exchange from  $\text{Cu}_3\text{Se}_2$  NCs.  $\text{Ag}_2\text{Se}$  nanocubes were obtained from the dropwise addition at room temperature of 0.08 mL of a 0.2 mM  $\text{AgNO}_3$  methanol solution to a toluene solution containing approximately 10 mg of  $\text{Cu}_3\text{Se}_2$  NCs.<sup>15</sup>

In summary, we described how  $\text{Al}^{3+}$  ions catalyzed the formation of  $\text{Cu}_x\text{Se}$  nanocubes. The composition of the obtained copper selenide nanocubes was identified as  $\text{Cu}_3\text{Se}_2$  and no aluminum was detected within the NC structure.  $\text{Cu}_3\text{Se}_2$  nanocubes showed a strong composition-dependent plasmonic peak in the wavelength range between 900 and 1100 nm.  $\text{Cu}_3\text{Se}_2$  nanocubes were also proven as an excellent platform for the production of other selenide nanocubes.

## ■ ASSOCIATED CONTENT

### Supporting Information

Detailed optimized conditions to obtain copper selenide nanocubes and EDX spectrum. This material is available free of charge via the Internet at <http://pubs.acs.org>.

## ■ AUTHOR INFORMATION

### Corresponding Author

acabot@irec.cat

### Notes

The authors declare no competing financial interest.

## ■ ACKNOWLEDGMENTS

The research was supported by the European Regional Development Funds. M.I. thanks the Spanish MICINN for her Ph.D. grant. J.A. and R.Z. also acknowledge MAT2010-15138.

## ■ REFERENCES

(1) (a) Catherine, J. M. *Science* **2002**, 298, 2139. (b) Song, H.; Kim, F.; Connor, S.; Somorjai, G. A.; Yang, P. D. *J. Phys. Chem. B* **2005**, 109, 188. (c) Sherry, L. J.; Chang, S. H.; Schatz, G. C.; Duyue, R. P. V.; Wiley, B. J.; Xia, Y. N. *Nano Lett.* **2005**, 5, 2034. (d) Xiong, Y. J.; Wiley, B. J.; Chen, J. Y.; Li, Z. Y.; Yin, Y. D.; Xia, Y. N. *Angew. Chem.* **2005**, 117, 8127.

(2) (a) Zhang, J.; Kumbhar, A.; He, J. B.; Das, N. C.; Yang, K. K.; Wang, J. Q.; Wang, H.; Stokes, K. L.; Fang, J. Y. *J. Am. Chem. Soc.*

**2008**, 130, 15203. (b) Zhang, J.; Yang, H. Z.; Yang, K. K.; Fang, J. Y.; Zou, S. Z.; Luo, Z. P.; Wang, H.; Bae, I.; Jung, D. Y. *Adv. Funct. Mater.* **2010**, 20, 3727.

(3) (a) Yin, Y.; Alivisatos, A. P. *Nature* **2005**, 437, 664. (b) Ibáñez, M.; Guardia, P.; Shavel, A.; Cadavid, D.; Arbiol, J.; Morante, J. R.; Cabot, A. *J. Phys. Chem. C* **2011**, 115, 7947. (c) Ibáñez, M.; Zamani, R.; Li, W. H.; Shavel, A.; Arbiol, J.; Morante, J. R.; Cabot, A. *Cryst. Growth Des.* **2012**, 12, 1085. (d) Li, W. H.; Shavel, A.; Guzman, R.; Garcia, J. R.; Flox, C.; Fan, J. D.; Cadavid, D.; Ibáñez, M.; Arbiol, J.; Morante, J. R.; Cabot, A. *Chem. Commun.* **2011**, 47, 10332.

(4) (a) Zhang, J.; Fang, J. Y. *J. Am. Chem. Soc.* **2009**, 131, 18543. (b) Zhang, J.; Yang, H. Z.; Fang, J. Y.; Zou, S. H. *Nano Lett.* **2010**, 10, 638.

(5) Wang, C.; Daimon, H.; Lee, Y.; Kim, J.; Sun, S. J. *Am. Chem. Soc.* **2007**, 129, 6974.

(6) (a) Lim, S. I.; Ojea-Jiménez, I.; Varon, M.; Casals, E.; Arbiol, J.; Puntès, V. *Nano Lett.* **2010**, 10, 964. (b) Chen, J. Y.; Lim, B.; Lee, E. P.; Xia, Y. N. *Nano. Today* **2009**, 4, 81.

(7) Loukrakpam, R.; Chang, P.; Luo, J.; Fang, B.; Mott, D.; Bae, I. T.; Naslund, R.; Engelhard, M. H.; Zhong, C. J. *Chem. Commun.* **2010**, 46, 7184.

(8) (a) Chen, J.; Herricks, T.; Xia, Y. N. *Angew. Chem., Int. Ed.* **2005**, 44, 2589. (b) Chen, J.; Herricks, T.; Geissler, M.; Xia, Y. N. *J. Am. Chem. Soc.* **2004**, 126, 10854. (c) Lim, B.; Lu, X.; Jiang, M.; Camargo, P. H. C.; Cho, E. C.; Lee, E. P.; Xia, Y. N. *Nano Lett.* **2008**, 8, 4043.

(9) Grass, M. E.; Yue, Y.; Habas, S. E.; Rioux, R. M.; Teall, C. L.; Yang, P.; Somorjai, G. A. *J. Phys. Chem. C* **2008**, 112, 4797.

(10) Teng, X.; Yang, H. *Nano Lett.* **2005**, 5, 885.

(11) Bullen, C.; van Embden, J.; Jasieniak, J.; Cosgriff, J. E.; Mulder, R. J.; Rizzardo, E.; Gu, M.; Raston, C. L. *Chem. Mater.* **2010**, 22, 4135.

(12) (a) Haram, S. K.; Santhanam, K. S. V.; Numann-Spallar, M.; Levy-Clement, C. M. *Res. Soc. Bull.* **1992**, 27, 1185. (b) Haram, S. K.; Santhanam, K. S. V. *Thin Solid Films* **1994**, 238, 21. (c) Heyding, R. D.; Murray, R. M. *Can. J. Chem.* **1976**, 54, 841.

(13) (a) Chen, W. S.; Stewart, J. M.; Mickelson, R. A. *Appl. Phys. Lett.* **1985**, 46, 1095. (b) Hermann, A. M.; Fabick, L. J. *Cryst. Growth* **1983**, 61, 658. (c) Okimura, H.; Matsumae, T.; Makabe, R. *Thin Solid Films* **1980**, 71, 53. (d) Riha, S. C.; Johnson, D. C.; Prieto, A. L. *J. Am. Chem. Soc.* **2011**, 133, 1383.

(14) (a) Deka, S.; Genovese, A.; Zhang, Y.; Miszta, K.; Bertoni, G.; Krahn, R.; Giannini, C.; Manna, L. *J. Am. Chem. Soc.* **2010**, 132, 8912.

(b) Dorfs, D.; Hartling, T.; Miszta, K.; Bigall, N. C.; Kim, M. R.; Genovese, A.; Falqui, A.; Povia, M.; Manna, L. *J. Am. Chem. Soc.* **2011**, 133, 11175. (c) Gurin, V. S.; Prokopenko, V. B.; Alexeenko, A. A.; Wang, S.; Prokoshin, P. V. *Mater. Sci. Eng., C* **2001**, 15, 93.

(d) Machado, K. D.; Lima, J. C.; Grandi, T. A.; Campos, C. E. M.; Maurmann, C. E.; Gasperini, A. A. M.; Souza, S. M.; Pimenta, A. F. *Acta Crystallogr., Sect. B* **2004**, 60, 282. (e) Jagminas, A.; Juskenas, R.; Gailiute, I.; Statkute, G.; Tomasiunas, R. *J. Cryst. Growth* **2006**, 294, 343. (f) Seoudi, R.; Shabaka, A. A.; Elokr, M. M.; Sobhi, A. *Mater. Lett.* **2007**, 61, 3451. (g) Hessel, C. M.; Pattani, V. P.; Rasch, M.; Panthani, M. G.; Koo, B.; Tunnell, J. W.; Korgel, B. A. *Nano Lett.* **2011**, 11, 2560.

(h) Luther, J. M.; Jain, P. K.; Ewers, T.; Alivisatos, P. A. *Nat. Mater.* **2011**, 10, 361. (i) Ibáñez, M.; Cadavid, D.; Zamani, R.; García-Castelló, N.; Izquierdo-Roca, V.; Li, W.; Fairbrother, A.; Prades, J. D.; Shavel, A.; Arbiol, J.; Pérez-Rodríguez, A.; Morante, J. R.; Cabot, A. *Chem. Mater.* **2012**, 24, 562.

(15) (a) Son, D. H.; Hughes, S. M.; Yin, Y. D.; Alivisatos, A. P. *Science* **2004**, 306, 1009. (b) Pietryga, J. M.; Werder, D. J.; Williams, D. J.; Casson, J. L.; Schaller, R. D.; Klimov, V. I.; Hollingsworth, J. A. *J. Am. Chem. Soc.* **2008**, 130, 4879.